Suppression of twins in *b*-oriented MFI molecular sieve films under microwave irradiation

Yi Liu,[a,b] Yanshuo Li*,[a] Rui Cai,[a] and Weishen Yang*,[a]

State Key Laboratory of Catalysis, Dalian Institute of Chemical Physics, Chinese Academy of Sciences, Dalian, 116023, China and Graduate School of Chinese Academy of Sciences, Beijing, 100039, China

E-mail: yangws@dicp.ac.cn, leeys@dicp.ac.cn

Supporting Information

SI-1. Experimental details

The detailed procedure for the preparation of compact and highly b-oriented MFI seed layer was described in our previous work (*J. Am. Chem. Soc.* **132**, *2010*, 1768). Unless otherwise specified, glass plates (2×2 cm^2) were used as substrates in experiment. The morphology of the prepared MFI seed layer was also shown in supporting information. The seed layer was then subject to secondary growth with the molar composition of synthetic solutions $5SiO_2$:1TPAOH:$1000H_2O$:20EtOH. With sequential addition of TEOS (98 %, Kermel) and TPAOH (20 wt.%, Aldrich) into DDI water, the mixture was further aged at 25 ^oC for 5 h. The precursor solution was then transferred to a Teflon-lined autoclave, in which the seeded substrate had been vertically placed. Consequently, secondary growth was initiated under desired conditions in a microwave reactor (MICROSYNTH, Milestone) with the maximum power output of 300 W. During microwave processing, sample temperature was measured by an optical fiber, which was immersed into the bottom of the reaction vessel. The actual temperature variation of the solution during the reaction coincided with the set temperature program very well. The mixture was heated from room temperature to 150 ^oC within 5 min. Microwave-assisted heating was initiated at 150 ^oC for 30 min to obtain a defect-free MFI film.

Conventional hydrothermal secondary growth was also initiated in our experiment. Both molecular composition and preparation procedure of the precursor solution were identical. Consequently, the vessel containing seed MFI layer and precursor solution was placed in a convective oven. The reaction was initiated at 150 ^oC for 5 h.

SI-2. XRC method for evaluating the regularity of *b*-oriented MFI grains

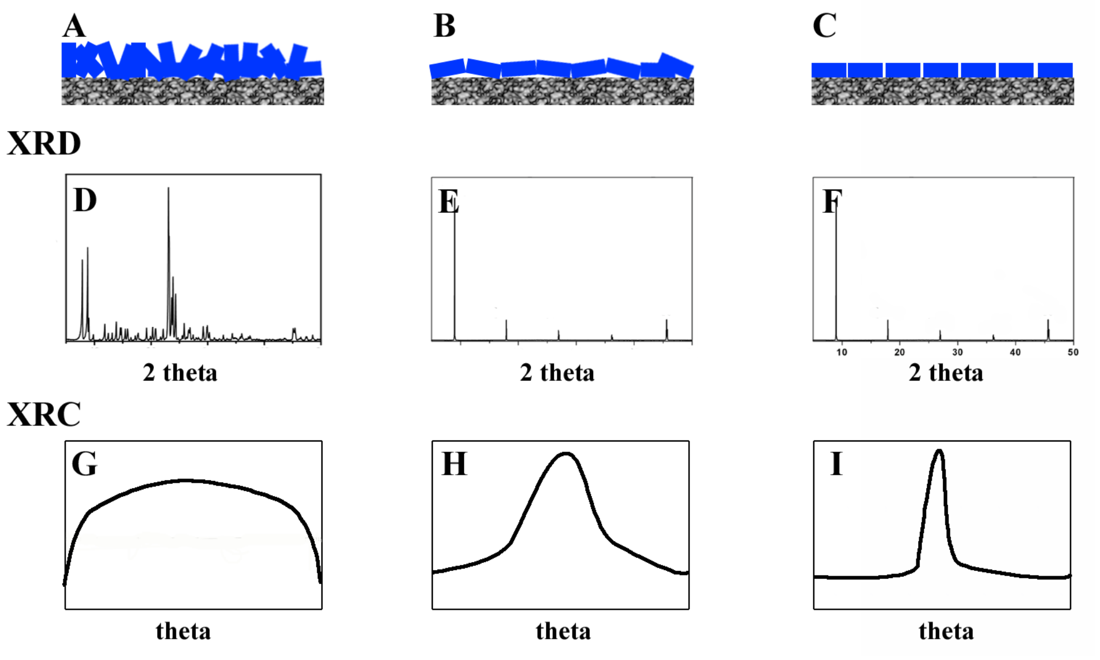

Fig. S1 Schematic illustration of the spatial arrangement of MFI grains on substrate: (A) randomly oriented MFI film, (B) *b*-oriented MFI film with low regularity and (C) *b*-oriented MFI film with high regularity. (D), (E), (F) were schematic XRD patterns of the above-mentioned MFI films, respectively. (G), (H), (I) were schematic XRC patterns of the above-mentioned MFI films with scanning angle (theta) around (0 2 0) diffraction peak.

Rocking curve measurements could be used as a gauge of the quality of crystalline film. It was made by doing a θ scan at a fixed 2θ angle, the width of which is inversely proportionally to the dislocation density in film.

Fig. S1 showed the influence of spatial arrangement of MFI grains on XRD and XRC patterns of different MFI films. In this study, XRC method was employed to investigate the regularity of *b*-oriented MFI grains on substrate. The degree of preferential *b*-orientation could be roughly evaluated by XRD technique (Fig. S1E, S1F), however, it was difficult to accurately characterize the dislocation density of *b*-oriented MFI grains. This issue could be solved with XRC method. Fig. S1H and S1I illustrated that the regularity of MFI grains directly determined the FWHM value of the theta scan peak profile. If MFI grains lay parallel to the substrate, the FWHM would be very narrow (Fig. S1I). On the contrary, even slight deviation between MFI grains and the substrate would lead to the widening of diffraction peak (Fig. S1H). However, this discrepancy could not be reflected in conventional XRD pattern.

SI-3. DSC method for monitoring nucleation

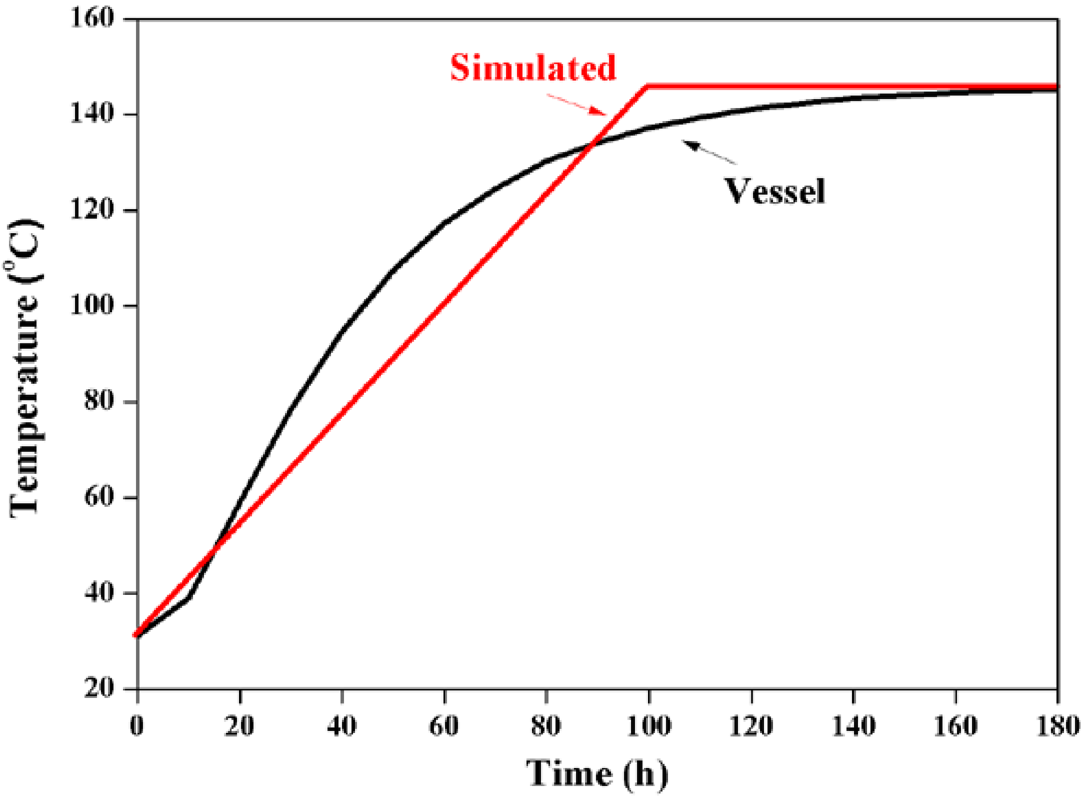

Fig. S2 Temperature data referring to DSC measurement. Black line: the actual temperature change in the Teflon-lined stainless steel autoclave. Red line: the programmed temperature change during the DSC measurement.

Fig. S2 illustrated the actual temperature change of precursor solution under conventional secondary growth. Although the temperature of oven had been set at 150 °C before the synthesis, after 3 hours, the temperature of solution could only reach 145 °C. While for microwave synthesis, the simulated temperature program and the actual temperature change in solution coincided with each other very well, which was not listed here.

DSC analyses were conducted with a high-pressure differential scanning calorimetry (Netzsch DSC 204 HP). Liquid samples were sealed in high-pressure sample crucible (chrome nickel steel, 27μl), which could withstand internal pressure up to 100 bar, and the temperature up to 500 °C. Au plates were used to seal the crucibles.

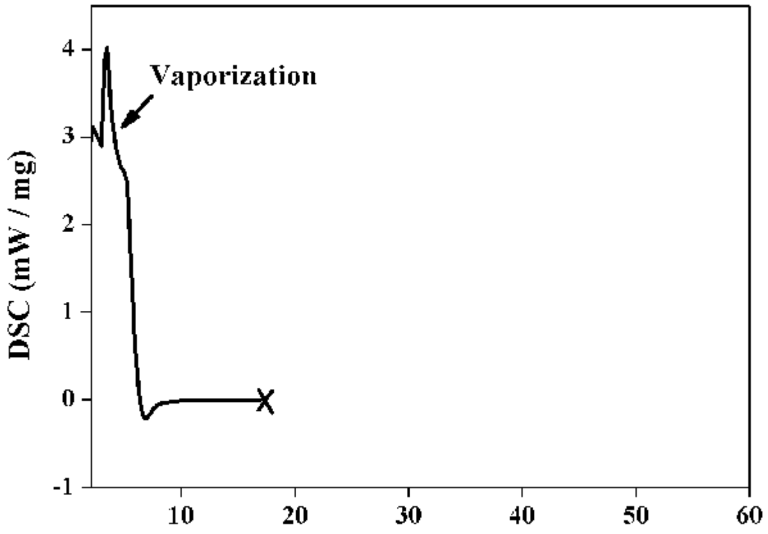

Fig. S3 DSC curve of simulated microwave-assisted synthesis. The component is pure water.

In Fig. 2c, an endothermic peak, which appeared at ~5 min, can be assigned to the enthalpy of water vaporization. The conclusion was further confirmed by the blank test (only pure water component existed during the test, as shown in Fig. S3) and previous report (*Langmuir*, *26*, **2010**, 5895). Combing results from Fig. 1c and Fig. S3, we came to the conclusion that new nucleation indeed did not happen before MFI film became compact.

SI-4. Microstructure evolution of nutrients in bulk solution under microwave-assisted heating and conventional heating

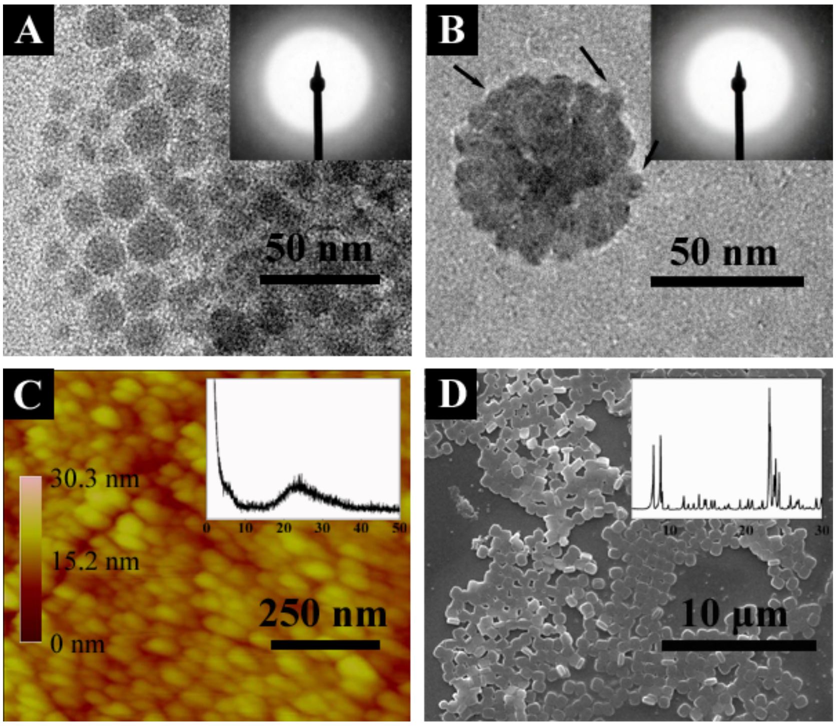

Fig. S4 TEM images of nanoparticles generated in the clear bulk solution after direct microwave heating at 150 °C for a) 10 min and b) 30 min. Insets: the selected area electron diffraction pattern of these nanoparticles. c) AFM pattern of nanoparticles formed at 150 °C for 30 min in bulk solution under microwave heating. d) SEM image of MFI crystals formed in bulk solution by conventional hydrothermal treatment at 150 °C for 2 h. Insets: XRD characterization of nanoparticles formed in the bulk under microwave-assisted heating and conventional hydrothermal growth.

For a deeper understanding of the nucleation bottleneck effect under microwave irradiation, the microstructural evolution of nanoparticles in bulk solution during secondary growth was investigated in detail (Fig. S4). After 10 min of microwave irradiation (shown in Fig. S4A), substantial nanoparticles (10~20 nm in size) were formed in bulk solution, as confirmed by transmission electron microscopy (TEM) and atomic force microscopy (AFM). The corresponding selected area electron diffraction (SAED) pattern (insets of Fig. S4A) revealed that they were predominantly amorphous. Further prolonging the synthesis time to 30 min (when a compact MFI film was formed) resulted in their compact agglomeration in the bulk solution (remaining amorphous, shown in Fig. S4B and S4C). In contrast, substantial MFI crystals (~1 µm in size) were generated in the bulk solution (2 h) under conventional secondary growth conditions before the MFI film became compact (Fig. S4D). These results strongly supported the fact that secondary nucleation in bulk solution exerted considerable influence on the growth behaviour of twin crystals on the MFI film during secondary growth. It should be noted here that although no nucleation occurred in the bulk solution during the microwave-assisted secondary growth, the new phases surrounding the MFI seeds were crystalline, as proved by glancing-incidence X-ray diffraction (GIXRD) In Fig. S5.

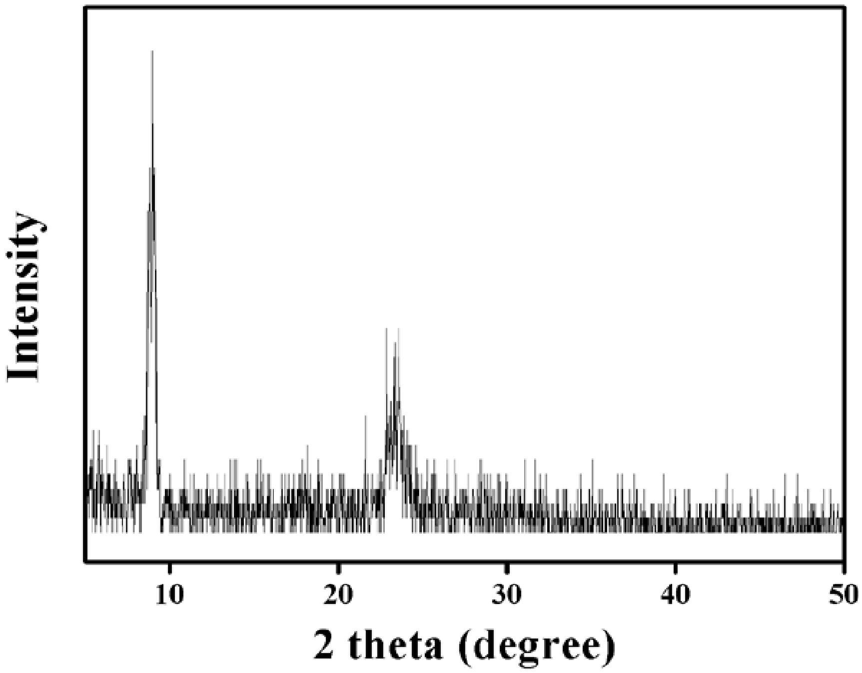

Fig. S5 GIXRD pattern of MFI film prepared by microwave-assisted secondary growth. Secondary growth conditions: at 150 °C for 10 min.

Fig. S5 showed the GIXRD pattern of MFI film grown under microwave irradiation. GIXRD technique provides a powerful tool to analyze the crystalline phase conditions of thin films. Here it was used to monitor the crystallinity of secondary growth portion grown on *b*-oriented MFI seed layer. The glancing incident angle was kept as low as 0.5 °, which guaranteed that the signal was mainly originated from the secondary growth portion. Results showed that the secondary growth portion preserved a high crystallinity, which was different from the amorphous nature of nanoparticles generated in bulk solution during secondary growth.

SI-5. Electrochemical characterization of the prepared MFI film

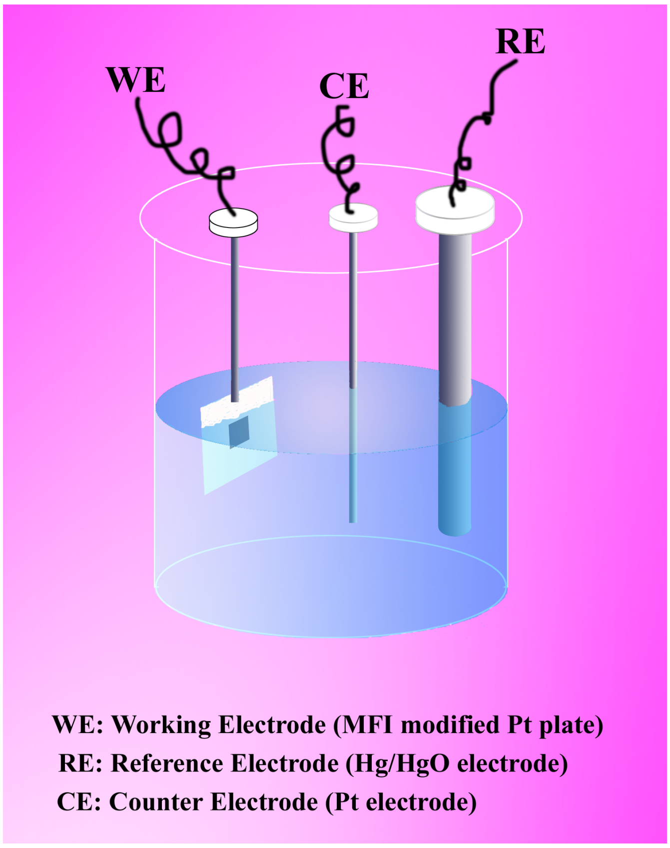

Fig. S6 Schematic illustration of the electrochemical systems used in the experiment.

Fig. S6 illustrated the electrochemical apparatus used in the experiment. Electrochemical data were obtained using a solartron 1287 instrument with computer data acquisition and control. Cyclic voltammetry (CV) experiments were performed in aqueous solutions with 0.5 M KCl as supporting electrolyte. CV responses of $[Fe(CN)_6]^{3-}$ were obtained with the concentration of 20 mM. Electrochemical measurements were conducted with a conventional three-electrode set up by using a Pt wire counter electrode and a saturated sodium calomel electrode (SCE) as a reference. MFI film-modified Pt plate was used as working electrode. The scanning voltage was set between -0.2 and 0.6 V, with the scan rate of 50 mV/s.

Linear sweep voltammetry (LSV) was performed in aqueous solutions with 0.1 M NaOH as supporting electrolyte. Responses of MeOH were obtained with the concentration of 0.6 M. Electrochemical measurements were conducted with a conventional three-electrode set up by using a Pt wire counter electrode and a saturated Hg/HgO electrode as a reference. MFI film-modified Pt plate was used as working electrode. The scanning voltage was set between -0.7 and 0.1 V, with the scan rate of 50 mV/s.

SI-6. Surface morphology and CV results of prepared MFI films

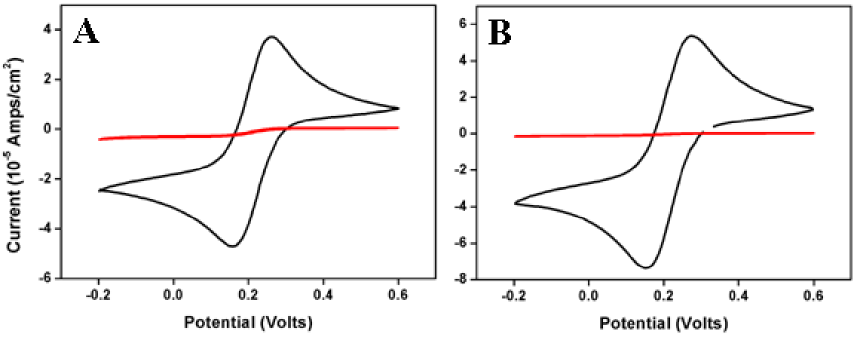

Fig. S7 Cyclic voltammograms of $[Fe(CN)_6]^{3-}$ aqueous solutions with (A) *b*-oriented MFI film-modified Pt plate as working electrode (red line). Black line: bare Pt electrode, and (B) *a*-&*b*-oriented MFI film-modified Pt plate as working electrode (red line). Black line: bare Pt electrode.

We verified the compactness of prepared MFI films by CV with $[Fe(CN)_6]^{3-}$ as probing molecules $[Fe(CN)_6]^{3-}$. Fig. S7A and S7B showed that there were no CV responses on both MFI film-modified Pt electrodes. As $[Fe(CN)_6]^{3-}$ (~7.2 Å) can not penetrate into the pores of MFI crystals along *b*-axis (~5.5 Å), results showed that no obvious intercrystalline defects existed in both MFI films.